View Article Online
View Journal

Dalton Transactions

An international journal of inorganic chemistry

Accepted Manuscript

This article can be cited before page numbers have been issued, to do this please use: S. K. Ramasamy and A. S.K. Kumar, *Dalton Trans.*, 2019, DOI: 10.1039/C9DT01830A.

ROYAL SOCIETY OF CHEMISTRY

rsc.li/dalton

View Article Online
DOI: 10.1039/C9DT01830A

ARTICLE

Light Activated CMP Conjugated 8-Aminoquinoline Turn-On Fluorescent Optode for Selective Determination of Th^{4+} in Aqueous Environment

Received 00th January 20xx,
Accepted 00th January 20xx

DOI: 10.1039/x0xx00000x

Selva Kumar R[a] and S.K. Ashok Kumar[a]*

A new dibutyl(2-oxo-2-(quinolin-8-ylamino)ethyl)phosphinate (**L**) was designed, synthesised and developed as a light active optode for Th^{4+} determination. The sensing performance of **L** was studied in solution as well as polymeric membrane phase using absorbance and emission techniques. The neutral ion carrier **L** exhibits weak fluorescence at 400 nm in CH_3CN:H_2O (9:1, v/v). Upon complexation of **L** with Th^{4+}, emission intensity at 486 nm was increased to 100-fold due to chelation induced enhanced fluorescence. The **L-Th^{4+}** binding interaction was studied by both Hill's and Job's plots. It indicates, the formation of complex species in 2:1 ratio with an estimated binding constant of 2.66 x10^4 M^{-2}. The complex formation between **L** and Th^{4+} was studied by NMR (^1H, ^{31}P), FTIR and LC-MS analysis. In order to make a probe for the sensing of Th^{4+} in 100% aqueous medium, the optode was prepared by immobilizing **L** as a neutral ion carrier in PVC support using dioctyl phthalate (DOP) as membrane solvent. The best performance of the optode was observed with a membrane composition of PVC:**L**:NaTPB:DOP in proportions of 35:5:3:57 (%, w/w) in the pH range 4.0-8.0. The optode can detect Th^{4+} concentration down to 1.1 nM with a fast response time of 15s and optical response remains unaltered even after 3 months; the optode sensing can be regenerated using Na_2EDTA solution. Finally, the optode was used for quantification of Th^{4+} in various water samples, monazite sand, and gas mantle samples.

Introduction

The progress of artificial optical receptors designed for the selective binding to actinides is an active area of research.[1–11] Particularly, thorium is an important metal for diverse applications such as the manufacture of ceramics, carbon arc lamps, and catalyst in the chemical industry,[12] its alloys are used in jet engine spare parts,[13] and in mantles for lanterns. It is also used as nuclear reactor fuels.[14] Due to the extensive use of Th[15,16] and its toxic properties, contamination of air, water, and soil components are likely. Hence, the development of simple and efficient techniques for the determination of thorium is most needed.[16] Many techniques have been used for determination of thorium such as ICP-MS,[17] ion chromatography, [18] neutron activation analysis,[19] voltammetry,[20] potentiometry,[21] radiometry,[22] X-ray fluorescence, [23] laser fluorescence,[24] alpha spectrometry,[25] and gamma spectrometry.[26] Yet, most of these techniques are expensive, skilled supervision and laborious procedure.[27]

Optical chemosensors with target-selective ligands and luminescent signaling systems for direct measurement of change in emission intensities arising upon analyte recognition have gained prime importance in current analytical research.[28] Numerous sensors were reported in the past few decades to detect various analytes, but most of them suffer to work in pure aqueous media which restrict their real applications.[29–32] Such a sensors can be applied in a fully aqueous medium with an additional advantage of reusability by developing a polymeric optode. In this system, immobilizing the sensing material (chromoionophores or fluoroionophores) with or without an extractant in the polymeric backbone support is a highly diversified method.[33–37]

Recently, some chromogenic and fluorogenic optodes for thorium have been reported using arsenazo III,[38] thorin,[39] xylenol orange,[40] triazene-1,3-di(2-methoxyphenyl),[41] 4-(p-nitrophenyl azo)–pyrocatechol,[42] and 2-(acetyloxy)-N-(5-nitro-2-thiazolyl)-benzamide[43] as sensing materials but some limitations such as poor sensitivity, limited working pH range, serious interference (Al^{3+}, UO_2^{2+}, Ti^{4+}, Zr^{4+}, and lanthanides) due to similar chemical properties need to be improved. Hence, the fabrication of highly selective optode for the quantification of Th^{4+} with good sensitivity to use under wide pH range and negligible interference from serious interfering ions are the main requirement for thorium sensor.[33,44,45]

Herein, ligand **L** was prepared by reacting 2-chloroquinolinyl acetamide with tributyl phosphate. As a part of our ongoing research on the development of new chemosensors for actinide ions,[35,46–48] the neutral carrier **L** was used for the fabrication of Th^{4+} selective polymeric optode and applied for the estimation of Th^{4+} in various samples.

[a] *Department of Chemistry, School of Advanced Sciences, Vellore Institute of Technology, Vellore-632014, Tamil Nadu, India.*
† E-mail: ashok312002@gmail.com.
Electronic Supplementary Information (ESI) available: [details of any supplementary information available should be included here]. See DOI: 10.1039/x0xx00000x

Experimental Section

Material and instruments

Dioctyl phthalate (DOP), polyvinyl chloride (PVC), sodium tetraphenylborate (NaTPB), 8-amino quinolone, tributyl phosphate, lanthanides as chloride salts, other metal ions as nitrate salts and required were purchased from Sigma Aldrich, SD fine and Merck chemicals.

Absorbance and emission spectral responses were recorded on a JASCO V-730 UV-Vis spectrophotometer and JASCO FP-8200 spectrofluorometer. Fluorescence lifetime measurement was carried using a HORIBA Jobin-Yvon instrument. FTIR spectra were recorded on a Shimadzu Affinity FTIR spectrometer in the range of 4000-400 cm^{-1}. NMR spectra were recorded using a 400 MHz Advance Bruker using TMS as an internal standard. Mass analysis was analysed using Agilent Ultivo LC/TQ. Spin coating carried out using Spin NXG-M1 manual spin coating unit.

Synthesis and characterization of L

The synthesis of **L** follows two steps reactions; in the first, preparation of intermediate product (2-chloro-N-(quinolin-8-yl)acetamide); in the second step, the reaction of intermediate product with tributyl phosphate, leading to the formation of final compound **L** (**Scheme 1**).

An intermediate product was synthesized by adding chloroacetyl chloride (0.8 mL, 1.2 eq.) dissolved in dry dichloromethane (DCM) which is slowly added to a stirred solution of quinoline-8-amine (1.16 g, 1 eq.) and triethylamine (0.3 mL) in DCM at 0 °C under nitrogen atmosphere. After the completion (as monitor by TLC), the reaction was quenched with saturated $NaHCO_3$ solution. The mixture was then extracted with 20 mL of DCM for about three times and the collected organic layer was washed with dil. HCl, dried with Na_2SO_4. The solvent was removed under reduced pressure, and the obtained residue was further purified by silica gel column chromatography (60-120 mesh silica gel, EA/Hex = 3:7). The obtained yield was 1.63g of 92%.

In the second step, the synthesized 2-chloro-N-(quinolin-8-yl) acetamide (1.10 g, 5mM) and tributyl phosphate (2 mL) were refluxed at 120 °C for overnight under nitrogen atmosphere.[49] The reaction progress was monitor by TLC. The obtained product was further purified by silica gel column chromatography (60-120 mesh silica gel, EA/Hex = 5:5) and the obtained yield was 1.61g of 85% yellow oily-liquid.

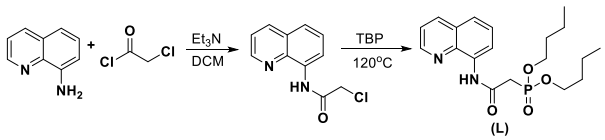

Scheme. 1. Reagents and conditions to synthesize **L**

2-chloro-N-(quinolin-8-yl) acetamide ($C_{11}H_9ClN_2O$): FTIR (ATR, cm^{-1}) 3269 (-NH), 2968 (-CH, Ar), 2899 (-CH, Ali), 1678 (C=O), 1240 (C-N) (**Fig. 1S**). ^{1}H NMR (400 MHz, DMSO-d_6) δ 10.91 (s, 1H), 8.87 (d *J* = 4.2, 1H), 8.75 (d *J* = 7.5 Hz, 1H), 8.19 (dd, *J* = 8.3, 1.3 Hz, 1H), 7.75 (d, *J* = 7.7 Hz, 2H), 7.49 (dd, *J* = 8.3, 4.2 Hz, 1H), 4.31 (s, 2H) (**Fig. 2S**). ^{13}C NMR (100 MHz, DMSO-d_6) δ 165.50, 149.57, 138.44, 137.44, 134.04, 128.36, 127.48, 123.28, 122.81, 117.43, 44.13 (**Fig. 3S**). DEPT 135 NMR (100 MHz, DMSO-d_6) δ positive 149.58, 137.44, 127.49, 123.28, 122.81, 117.44 and negative 44.13 (**Fig. 4S**). HR-MS (M^+) calculated: 220.0403 and obtained: 220.0400 (**Fig. 5S**).

L: ($C_{19}H_{27}N_2O_4P$): FTIR (ATR, cm^{-1}) 3336 (-NH), 2958 (-CH, Ar), 2873 (-CH, Ali), 1685 (C=O), 1527 (P=O), 1246 (N-C), 1018 (P-O) (**Fig. 6S**). ^{1}H NMR (400 MHz, $CDCl_3$) δ 10.40 (s, 1H), 8.84 (d, *J* = 4.2, Hz, 1H), 8.76 – 8.72 (m, 1H), 8.16 (dd, *J* = 8.3, 1.5 Hz, 1H), 7.53 (d, *J* = 4.2 Hz, 1H), 7.46 (dd, *J* = 8.3, 4.2 Hz, 1H), 7.44 (d, *J* = 4 Hz, 1H) 4.20 – 4.13 (m, 4H), 3.23 (d, *J* = 21.2 Hz, 2H), 1.73 – 1.64 (m, 4H), 1.38 (m, 4H), 0.87 (t, *J* = 7.4 Hz, 6H) (**Fig. 7S**). ^{13}C NMR (100 MHz, $CDCl_3$) δ 162.71, 148.37, 138.51, 136.25, 134.44, 127.93, 127.25, 121.96, 121.65, 116.79, 66.68, 66.62, 38.11, 36.81, 32.46, 32.39, 18.66, 13.56 (**Fig. 8S**). ^{31}P NMR (162 MHz, $CDCl_3$) δ 21.47 (**Fig. 9S**). DEPT 135 NMR (100 MHz, $CDCl_3$) δ Positive 148.37, 136.27, 127.25, 121.98, 121.65, 116.81, 13.56 and negative 66.70, 66.63, 38.10, 36.80, 32.45, 32.39, 18.66 (**Fig. 10S**). HR-MS (M^+): calculated: 378.1708 and obtained: 378.1705 (**Fig. 11S**).

Quantum yield

Fluorescence quantum yield of **L** and **L-Th^{4+}** was carried out as per the Nature method reported by Resch-Genger.[50] The standard compound quinine sulfate was used and it's quantum yield is 0.546 in 0.5 M H_2SO_4.[51] In order to calculate quantum yield, the UV-Vis absorbance and emission spectra of five different concentrations of quinine sulfate, **L** and **L-Th^{4+}** were taken in acetonitrile. Further, the quantum yield was calculated using the equation (i).

$$\Phi_{f,s} = \Phi_{f,r}\,(F_s/F_r) \times (f_r/f_s)\,(\eta_s^2)(\lambda_{em})/(\eta_r^2)(\lambda_{em})\text{----(i)}$$

Where s and r, denoted as sample (**L**, **L-Th^{4+}**) and reference quinine sulfate respectively. F_s and F_r is the integral photo flux and f_s and f_r are the absorption factors of sample and reference and η is the refractive index of the solvent.

Fabrication of optode

The PVC-based optode was prepared by thorough mixing of **L** (0-6%, w/w), NaTPB (0-6%, w/w), DOP (65-53%, w/w) and PVC (35%, w/w) for 200 mg batch added slowly in 2 mL of tetrahydrofuran (THF) in a 50 mL beaker to get complete homogenous mixture. Then, the mixture was allowed to evaporate at room temperature to remove the excess of THF solvent to get a consistent viscous solution. To improve the adhesion of the membrane on the quartz plate was activated by washing with concentrated nitric acid for 12 h followed by hydrofluoric acid (3%) and hydrogen peroxide (10%) each for 30 min, then washed with distilled water and ethanol. The mixture (100µL) was placed using micropipette on a quartz plate of dimension: 16 mm (l) x 12 mm (w) x 3 mm (t), the quartz plate was placed on a spin-on device and rotated at 2000 rpm for about 2 min to achieve uniform distribution of the membrane matrix on the quartz plate. The quartz plate coated with the polymeric membrane was taken out from the spin-on device and allowed to stand at ambient condition for 1 h before use.

The fluorescence measurement was carried out by keeping the quartz plate in a quartz cuvette cell containing 2 mL of pH 6.5 Tris-HCl buffer solution.[52] To this solution, Th^{4+} was added and corresponding emission intensity was recorded at 486 nm by exciting at 315 nm.

Fluorescence titration

The fluorescence titration was carried out to check the sensitivity of the optode-10 sensor by keeping the optode-10 diagonally inside quartz cuvette containing 2 mL of pH 6.5 tris-HCl buffer solution. To this solution an incremental amount of Th^{4+} (1 mM) was added using micropipette. After each addition of Th^{4+}, emission spectra was recorded upon excitation at 315 nm

Response time determination

The optode response time was carried out by using the optode-10 placing diagonally inside cuvette cell containing in 2 mL buffer solution. To this solution added 20 µM of Th^{4+} solution and the fluorescence intensity at 486 nm was recorded at every 2 seconds time interval upon an excitation at 315 nm.

Estimation Th^{4+} in water samples

Initially, the 1 mM Th^{4+} stock solution was prepared by using double distilled water, tap water and well water collected from VIT University campus. The optode-10 sensor was immersed in 2 mL of buffer solution, to this solution added known amount of Th4+ solution. The emission intensity at 486 nm was recorded upon the excitation at 315 nm for all spiked samples. The spiked concentration of Th^{4+} was calculated using the calibration curve obtained using standard solution of Th^{4+} using same optode sensor.

Results and discussion

In order to establish selective polymeric optode for Th^{4+}, **L** is systematically characterized in solution phase using absorption and emission techniques.

UV-Visible and fluorescence spectral response of L

The metal binding ability of **L** (50 µM), the colorimetric changes of **L** were performed with twenty three different metal ions such as Na^{+}, Ca^{2+}, Mg^{2+}, Cr^{3+}, Mn^{2+}, Fe^{3+}, Co^{2+}, Ni^{2+}, Cu^{2+}, Zn^{2+}, Cd^{2+}, Hg^{2+}, Ag^{+}, Al^{3+}, In^{3+}, Bi^{3+}, Pb^{2+}, La^{3+}, Ce^{3+}, Lu^{3+}, Gd^{3+}, Sm^{3+}, Zr^{4+}, Ti^{4+}, UO_2^{2+} and Th^{4+} (10 eq.) in CH_3CN:H_2O (9:1, v/v) shown in **Fig. 1a**. Under visible light, a very weak colour changes of colourless to pale yellow was noticed with Al^{3+} and UO_2^{2+}. But, under UV light, the selective cyan colour fluorescence was noticed with Th^{4+} and slight yellow-orange fluorescence was noticed with Ti^{4+} and Zr^{4+}. While other tested metal ions, it did not give such visible changes under similar conditions.

The UV-Vis spectral studies of **L** (50 µM) shows two absorption maximum at 240 nm and 315 nm with a molar absorptivity of $2.0x10^4$ and $4.0x10^3$ $L.M^{-1}.cm^{-1}$, respectively (**Fig. 2a**). Both absorbance peaks are due to π-π* and n-π* transitions on the quinoline ring system. When **L** interacts with Th^{4+}, both peaks are experiencing a blue shift to 233 nm and 310 nm with a molar absorptivity of $1.65x10^4$ and 3.94 $x10^3$ $L.M^{-1}.cm^{-1}$ respectively (**Fig. 12S**). In order to check the sensitivity of the response, UV-Vis titration of **L** with Th^{4+} was carried out. The absorbance peak at 240 nm starts to undergo blue shift with slight hypochromic shift and band at 315 nm undergo slight hyperchromic shift with a clear isosbestic point at 238 nm, 310 nm, and 345 nm, which clearly indicated the new species formation during the interaction (**Fig. 2b, 13S**). Due to the low molar absorption coefficient of **L-Th^{4+}** complex, the quantification of Th^{4+} using **L** at low concentration becomes uncertain. However, **L-Th^{4+}** exhibits emission property shown **Fig.1b**.

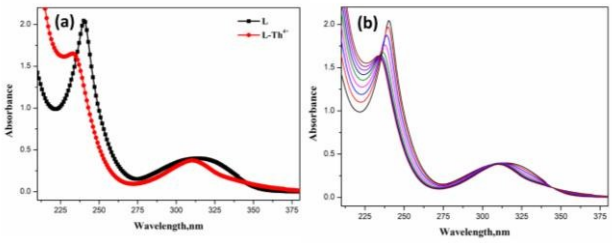

Fig. 2. (a) UV-Vis spectral response of **L** (50 µM) and **L-Th^{4+}**(2eq.) in CH_3CN:H_2O (9:1, v/v) (b) UV-Vis spectral titration of **L** (50µM) with Th^{4+} (0-2 eq.) in CH_3CN:H_2O (9:1, v/v).

In order to study fluorescence properties of **L** and its complex, emission spectra were recorded for **L** in the presence and absence of different metal ions in CH_3CN:H_2O (9:1, v/v) media by exciting at 315 nm. Accordingly, alone **L** shows a weak emission band at 400 nm. However, **L** shows a strong emission band at 486 nm upon interaction with Th^{4+} while Ti^{4+}, Zr^{4+} exhibits a weak emission intensity to an extent of 10-fold increase while for other metal ions, emission intensity increased to a factor of 3-4 fold (**Fig. 3a**). Besides, a large Stokes shift (171 nm) (**Fig. 3b**) and intensity increased by 100-fold with Th^{4+} (15au to 1500 au). On excitation of **L** and its metal complexes at 240 nm, **L** did not show any emission band while complexes of Ti^{4+},

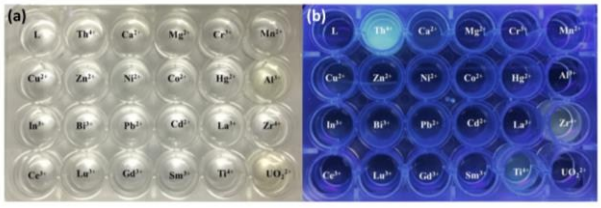

Fig. 1. Colorimetric performance of **L** (50 µM) with various metal ions (10 eq.) under (a) visible light (b) UV light.

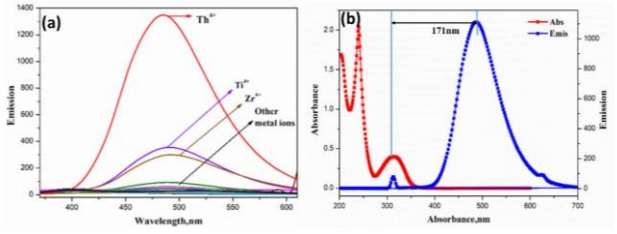

Fig. 3. Fluorescence response of **L** (50 µM) with (a) various metal ions (10 eq) upon the excitation at 315 nm (b) Absorbance and emission spectral response of **L-Th^{4+}** in CH_3CN:H_2O (9:1, v/v).

Zr^{4+}, and Th^{4+} showed weak emission intensity at 486 nm. Hence, all sensing ability of **L** with selected metal ions were studied by exciting at 315 nm (**Fig. 14S**).

The non-fluorogenic nature of **L** is due to the photoinduced electron transfer (PET) occurred from a phosphoryl oxygen to the quinoline ring system (**Scheme 2)**.[53,54] In the case of **L-Th^{4+}** complex, the significant fluorescence enhancement of **L** is due to the participation of carbonyl oxygen, phosphoryl oxygen, and quinoline nitrogen in coordinate bond formation with Th^{4+} which triggered inhibits the PET process.[55]

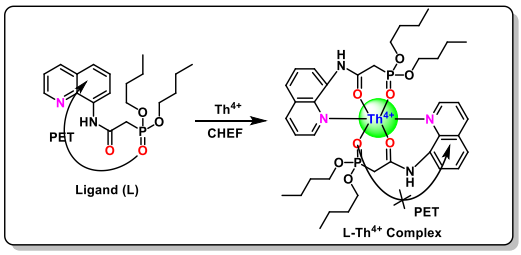

Scheme 2 The possible mechanism of fluorescence in **L** and **L-Th^{4+}**

To elucidate the sensitivity of **L** towards Th^{4+}, spectral titration was carried out by sequential addition of Th^{4+} to a fixed quantity of **L** and measured emission intensity at 486 nm (**Fig. 4a, 15S**). The titration data reveals that linear correlation between the concentrations of Th^{4+} and a measured intensity in the range of 1-25 µM of Th^{4+}. The binding stoichiometric ratio of **L** with Th^{4+} was determined by using Job's plot [56] by maintaining the sum of the concentrations of Th^{4+} and **L** constant and varying the molar ratio of Th^{4+} from 0.1 to 0.9. As seen in **Fig. 4b**, it shows that when a molar fraction of Th^{4+} reached 0.3, it exhibits maximum intensity which reflects a 2:1 stoichiometry between **L** and Th^{4+}. Further to support Job's method, the binding stoichiometry was calculated using Hill's plot[57,58] shown in **Fig. 4c**. The slope calculated to be 2.085 indicating the involvement of 2**L** binding with Th^{4+}. The binding constant was calculated from the fluorescence titration data using a non-linear curve fitting of 2:1 binding model on BindFit v0.5 program. The estimated association constant was found to be 2.66 x10^4 M^{-2} (**Fig. 4d**).

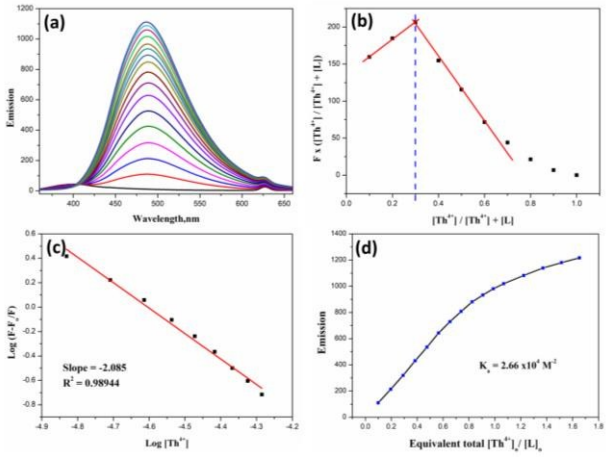

Fig. 4. (a) Fluorogenic titration of **L** (50 µM) Th^{4+}(0-30 µM) Binding stoichiometric study using (b) Job's plot (c) Hill's plot (d) BindFit plot in CH_3CN:H_2O (9:1, v/v) (λ_{ex} = 315 nm and λ_{em} = 486 nm).

The quantum yield of **L** and **L-Th^{4+}** was calculated by standard procedure and it was found to be 0.103 and 0.274, respectively. In order to establish fluorescence properties of **L** and **L-Th^{4+}**, time-resolved fluorescence decay measurements were performed to calculate lifetime (1.27 ns and 3.47 ns), radiative decay process (K_r= 8.11 x10^7 s^{-1}) and non-radiative (K_{nr}= 70.6 x10^7 s^{-1}) for **L** and decay process (K_r= 7.89 x10^7 s^{-1}) and non-radiative (K_{nr}= 20.9 x10^7 s^{-1}) for **L-Th^{4+}** respectively (**Fig. 5a**, **5b**). Results show that **L-Th^{4+}**complex exhibits an increase in K_r and decrease in K_{nr} recommends strong fluorescence emission associated with **L-Th^{4+}** complex.

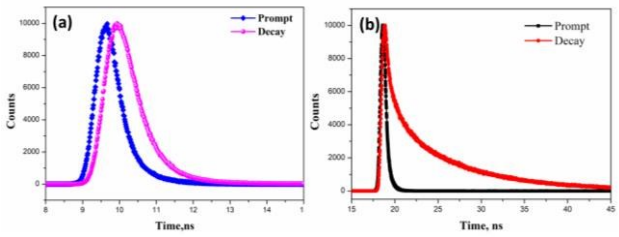

Fig. 5. Fluorescence lifetime decay profile of (a) **L** (50 µM, λ_{ex}= 315 nm and λ_{em} = 400 nm) and (b) **L-Th^{4+}** complex (50 µM, λ_{ex} = 315 nm and λ_{em} = 486 nm) in CH_3CN.

Performance of optodes

Any sensor works completely in the water phase and reusability always good for the sensor. These features encourage us to develop and characterize the optode sensor for Th^{4+} determination. The fluorescent optode used in this study is based on the immobilization of **L** in a plasticized PVC containing NaTPB as a lipophilic anionic additive. Since **L** is neutral ion carrier and co-agent (NaTPB) lipophilic anions provide ion-exchange properties to optode membrane.[32,33] The possible response mechanism of the present optical sensor can be supported by the following ion-exchange mechanism shown in equ-ii.[59,60]

$$Th^{4+}_{(aq)} + L_{(org)} + NaTPB_{(org)} \rightleftharpoons L\text{-}Th_{(org)} + TPB_{(org)} + Na^{+}_{(aq)} + NO_3^{-}{}_{(aq)} \text{---(ii)}$$

For the preparation of an ion-selective optical sensor, the ligand **L** will be incorporated into a hydrophobic membrane such as a plasticized PVC membrane. Then, the sensor is used in contact with a solution containing a primary ion (Th^{4+}). This ligand **L** can extract Th^{4+} from aqueous solution into the organic membrane phase and form a complex which exhibits fluorescence emission at 486 nm. As can be seen from **Fig. 6a**, the fluorescence intensity of the optode membrane increases with increasing concentration of Th^{4+}, which constitutes the basis for the determination of Th^{4+}. Various membranes were prepared by dissolving various membrane ingredients (in % weight) such as **L** (0-6), DOP (55-65), NaTPB (2-6) and PVC (35) in 2 mL of THF. The total membrane composition was fixed to 200 mg. The ratio of **L** and different membrane ingredients were optimized to give a better response in terms of working concentration range, and response time. From **Table 1**, it is clear that as the amount of **L**

View Article Online
DOI: 10.1039/C9DT01830A

Table 1. Optimization of optode membrane ingredients

S.No.	PVC (%, w/w)	DOP (%, w/w)	L (%, w/w)	NaTPB (%, w/w)	Working Range (M)	Response Time (s)
1	35	65	-	-	No response	-
2	35	64	1	-	1×10^{-5} to 5×10^{-3}	60
3	35	63	2	-	8×10^{-6} to 10×10^{-5}	22
4	35	62	3	-	1×10^{-6} to 2.5×10^{-4}	35
5	35	61	4	-	5×10^{-7} to 1×10^{-4}	25
6	35	60	5	-	5×10^{-8} to 2.5×10^{-5}	30
7	35	59	6	-	1×10^{-7} to 2.5×10^{-5}	25
8	35	59	5	1	8×10^{-7} to 1×10^{-5}	35
9	35	58	5	2	5×10^{-8} to 2.5×10^{-5}	20
10	**35**	**57**	**5**	**3**	**2×10^{-9} to 5×10^{-4}**	**15**
11	35	56	5	4	1×10^{-8} to 2.5×10^{-5}	20
12	35	55	5	5	5.5×10^{-9} to 1.5×10^{-5}	25

increases from 0 to 6 %, optical response of optode also increases and attained highest sensitivity at 5% of **L**. Further, the effect of lipophilic salt on **L** carried out from 0 to 6%, results show that at 3%, the optode gave the best response in terms of detection limit (1.1 nM) and response time (15s) (**Fig. 16S**).[33] The absence of lipophilic salt affects the working concentration range and delay the fluorescence response. Furthermore, all other studies were carried out using optode-10. As shown in **Fig. 6a**, the free optode shows no fluorescence emission upon the complexation with Th^{4+} it shows remarkable fluorescence change. The lowest detection limit (LOD) and lowest detecting quantity (LOQ) was calculated according to IUPAC definition using the linear equation obtained from calibration plot (**Fig. 6b**).[61] The LOD and LOQ were found to be 1.1 nM and 3.69 nM respectively. The membrane optode was regenerated by treating with a strong chelating agent such as Na_2EDTA. The Th^{4+}-EDTA complex stability constant was comparatively high, so it is expected to easily decomplex the **L-Th^{4+}** complex and leaves the free neutral carrier **L** in the membrane phase. For subsequent Th^{4+} measurements, the optode should be kept in a pH 6.5 buffer solution for about 10 min (**Fig. 17S**). To calculate the lifetime of the optode-10, every ten days of time interval, fluorescence response was recorded and plotted calibration graph to find the detection limit. The result reveals that the detection limit of Th^{4+} does not change till 90th day use. After 90th day, the response of the optode start to decrease (**Fig. 18S**). This shows that optode can used for about 3 months.

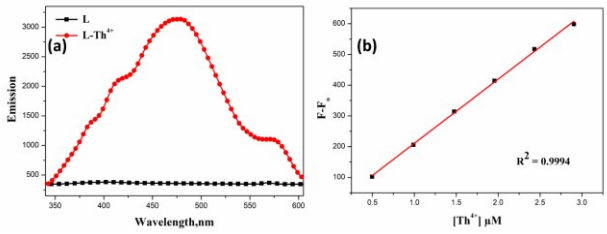

Fig. 6. (a) Fluorescence response of optode-10 with and without Th^{4+} (25µM) in pH 6.5 buffer (b) Calibration curve (λ_{ex} = 315 nm and λ_{em} = 486 nm).

Effect of pH

The response of pH on fluorescence intensity of optode-10 studied in the presence and absence of Th^{4+} (20 µM). The required pH 1.0- 12.0 adjusted using 0.1N HCl/NaOH solution. The emission intensity was recorded at 486 nm upon excitation at 315 nm. As seen from **Fig. 7**, fluorescence intensity remains same in the pH range 4-8 and above pH 8 and below pH 4 decreased due to formation polymeric thorium hydroxide formation $Th_x(OH)_y$.[62] and protonation of heteroatoms. However, in the case of free optode, it didn't give any change in fluorescence intensity by varying the pH from 1.0 to 12.0 due to the non-fluorogenic nature of **L**.

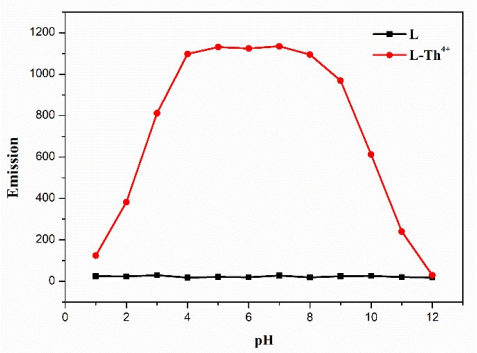

Fig. 7. Effect of pH on the performance of optode-10 and optode with 20 µM of Th^{4+} in various buffer solutions (λ_{ex} = 315 nm and λ_{em} = 486 nm).

Interference study

The specificity of optode-10 as a probe for the quantification of Th^{4+} (0.5 eq) in the presence of various interfering metal ions (5 eq.) was explored in a fully aqueous medium. The emission intensity was recorded at 486 nm upon excitation at 315 nm. As seen from **Fig. 8**, the intensity of optode in the presence of Th^{4+} is unperturbed in the presence of 10 eq. of interfering ions; this Indicates an excellent selectivity of Th^{4+} over competing ions. The response of optode-10 for Th^{4+} detection in the presence of UO_2^{2+}, Ce^{3+}, Al^{3+}, and group IV-B elements such as Ti^{4+} and Zr^{4+}

View Article Online
DOI: 10.1039/C9DT01830A

Table 2. Fluorogenic optode performance towards Th^{4+} recognition and its comparison with previously reported work.

Name of chromogenic/fluorogenic ionophore	Matrix	Mode	Response Time (s)	λ_{max} (nm)	LOD	pH	Interference
4-(p-nitrophenyl azo)–pyrocatechol[37]	PVC	Abs	600	500	6 µM	3.5	Ga^{3+}, UO_2^{2+}
Triazene-1,3-di(2-methoxyphenyl)[41]	PVC	Abs	60	370	1.15 µM	3.0	UO_2^{2+}
Arsenazo III[38]	PEI-PCMs	Abs	30	540	2.6 µM	3.0	NR
Thorin[38]	PEI-PCMs	Abs	50	483	2.7 µM	3.0	NR
Thionin[38]	PEI-PCMs	Abs	60	606	0.97 µM	6.0	NR
Thorin–methyltrioctylammonium[39]	CTA	Abs	420	554	1.85 µM	3.0	La^{3+}, As^{3+}, Sb^{3+}
2-(acetyloxy)-N-(5-nitro-thiazolyl)-benzamide[43]	Sol-gel	Em	120	420/482	78 nM	4.0	NR
Xylenol orange[40]	PAN	Abs	600	576	0.2 µM	4.0	NR
L (Present work)	PVC	Em	15	315/486	1.1 nM	6.5	No Interference

NR- not reported, PEI -polyethylenimine, PCMs -pluronic polycarbamates, CTA-cellulose triacetate, PAN-polyacrylonitrile, Abs-absorbance and Em -emission.

is relatively low but clearly, quantification can be made (**Fig. 8a**). Further, the effect of selected anions response was investigated and results indicate that there is no significant change in intensity in the presence of other anions (**Fig. 8b**). In **Table 2**, the present optode was compared with the previously reported Th^{4+} selective optodes.[21–26] The present optode is significantly improved in terms of response time, detection limit and interference.

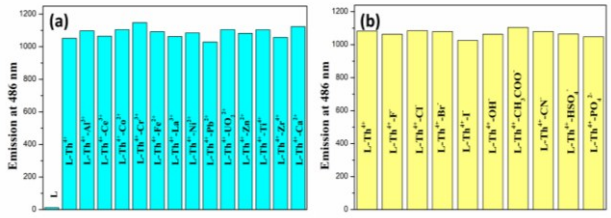

Fig. 8. Bar diagram representing performance of optode-10 with 20µM of Th^{4+} in the presence of various (a) metal ions (100 µM) (b) anions (100 µM) in pH 6.5 buffer (λ_{ex} = 315 nm and λ_{em} = 486 nm).

Sensing mechanism

The binding mechanism of **L** with Th^{4+} was studied by recording the ^1H, ^{13}C and ^{31}P NMR for neat **L** and **L-Th^{4+}** complex in DMSO-d_6. As seen in **Fig. 9a**, neutral carrier **L** alone exhibits amide (N-H) peak at 10.36 ppm and bridging methyl (-CH_2) at 3.52 ppm. When **L** interacted with Th^{4+}, amine (N-H) peak experience deshielding effect (at 10.41 ppm) whereas bridging methyl (CH_2) experience shielding effect (at 3.46 ppm). The ^{13}C NMR spectra for **L** shows (**Fig. 9c**), the carbonyl carbon peak at 163 ppm, upon complexation with Th^{4+}, the carbonyl peak exhibits as two signals with small deshielding effect (at 164 ppm). The splitting of the carbonyl carbon signal suggests that the carbonyl groups are in the **L-Th^{4+}** complex are an unsymmetrical environment of distracted octahedron geometry.

The ^{31}P NMR spectra of **L** and **L-Th^{4+}** given in **Fig. 9b**, here, **L** alone exhibits a peak at 22.39 ppm, which experience shielding effect (21.60 ppm) upon complexation with Th^{4+}. Overall, the change in NMR signal suggests that the **L** binds with Th^{4+} through coordination of phosphoryl oxygen (P=O), carbonyl carbon (C=O), and with quinoline nitrogen (-N=). Further, as seen in **Fig. 9d**, the FTIR spectra of neat **L** shows peak at 3336 cm^{-1} for amide ν_{N-H}, 2958 cm^{-1} for aromatic ν_{C-H}, 2874 cm^{-1} for aliphatic ν_{C-H}, carbonyl (C=O) 1682 cm^{-1} for the $\nu_{C=O}$, imine (-N=) 1527 cm^{-1} for $\nu_{C=N}$, phosphine oxide (P=O) 1246 cm^{-1} for $\nu_{P=O}$, 975 cm^{-1} for ν_{P-O-C} stretching and 556 cm^{-1} for ν_{P-O-C} bending vibrations. After interacting with Th^{4+}, it exhibits all peaks are experiencing shifts from the original vibrations. Accordingly

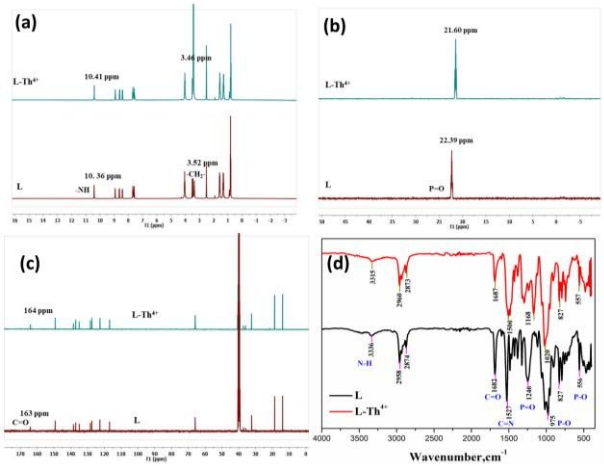

Fig. 9. Establishment of binding mechanism of **L** with Th^{4+} using (a) ^1H NMR (b) ^{31}P NMR (c) ^{13}C NMR for **L** and **L-Th^{4+}** complex in DMSO-d_6 (d) FTIR spectra.

shifted to 3315 cm^{-1} for amide ν_{N-H}, 2960 cm^{-1} for aromatic ν_{C-H}, 2873 cm^{-1} for aliphatic ν_{C-H}, 1687 cm^{-1} for the $\nu_{C=O}$, 1506 cm^{-1} for $\nu_{C=N}$, 1168 cm^{-1} for $\nu_{P=O}$, 1020 cm^{-1} for ν_{P-O-C} stretching and 557 cm^{-1} for ν_{P-O-C} vibrations. The FTIR study reveals the participation of C=O, P=O and -N=C are involved in the bond formation with Th^{4+}.

Further, LC-MS analysis of **L-Th** complex exhibits two major peaks appeared at 1006.4204 (m/z) and 1011.3639 (m/z) which corresponds to species involvement of 2**L**+1Th+NH_4^+ and 2**L**+1Th+Na with a calculated mass of 1006.4114 (m/z) and 1011.3695 (m/z) respectively (**Fig. 19S**). Finally, LC-MS analysis also supporting the formation of 2:1 ligand to metal complex.

Analytical applications

The practical utility of the optode-10 was studied to estimate the Th^{4+} concentration in different water samples such as double distilled water, bore well water and well water. The results are given in **Table 3**, it shows good agreement between the spiked and recovered concentration of the thorium. Besides, the same optode was successfully used for the direct quantification of thorium in monazite sand and lantern gas mantle samples and results are compared with ICP-MS analysis. As it is clear from **Table 3**, there is a satisfactory agreement between the thorium detected by optode-10 and those determined with the ICP-MS method.

Table 3. Analysis of Th^{4+} in different water systems and real sample analysis using optode-10

Name of the samples	Th^{4+} added (μg/mL)	Th^{4+} found (μg /mL)	Precision (%)
DD water	50	49.45 ± 0.14	98.90
	100	98.70 ± 0.51	98.70
Tap water	50	48.54 ± 0.17	97.08
	100	98.14 ± 0.43	98.14
Well water	50	47.84 ± 0.04	95.68
	100	96.52 ± 0.16	96.52
Monazite sand	8.62[a]	8.52 ± 0.09	98.83
Gas mantle	2.41[a]	2.37 ± 0.15	98.34

[a] Thorium amount estimated from ICP-MS analysis

Conclusion

A new fluorogenic optode for the selective detection of Th^{4+} in fully aqueous medium was developed. The optode can work in the pH range of 4-8 with a LOD of 1.1 nM and response time of 15s. The optode exhibits no interference from other tested cations and anions. The optode can be regenerated using Na_2EDTA and works for 3 months without any change. The present optode exhibits a good selectivity, quick response time, reproducibility, detection limit and the performance of the optode was used to detect Th^{4+} in different samples. Hence, it can be ranked best optode compare to reported optodes in the literature.

Conflicts of interest

There are no conflicts to declare.

View Article Online
DOI: 10.1039/C9DT01830A

Acknowledgements

Authors thank Board of Research in Nuclear Sciences (BRNS), GOI for supporting the work through the project grant (34/14/11/2015/BRNS). Authors are also thankful to DST-VIT-FIST for NMR and Vellore Institute of Technology, Vellore for other research facilities

Notes and references

1 Z. Wang, N. Pu, Y. Tian, C. Xu, F. Wang, Y. Liu, L. Zhang, J. Chen and S. Ding, *Inorg. Chem.* 2019, **58**, 5457-5467.
2 C.L. Xiao, C.Z. Wang, L.Y. Yuan, B. Li, H. He, S. Wang, Y.L. Zhao, Z.F. Chai and W.Q. Shi, *Inorg. Chem.*, 2014, **53**, 1712–1720.
3 S. Dolai, S. K. Bhunia, L. Zeiri, O. Paz-Tal and R. Jelinek, *ACS Omega*, 2017, **2**, 9288–9295.
4 M. W. Peters, E. J. Werner and M. J. Scott, *Inorg. Chem.*, 2002, **41**, 1707–1716.
5 A. E. V Gorden, J. Xu, K. N. Raymond and P. Durbin, *Chem. Rev.*, 2003, **103**, 4207–4282.
6 G. J.P. Deblonde, A. Ricano and R. J. Abergel, *Nat. Commun.*, 2019, **10**, 2438.
7 S. Nagl and O. S. Wolfbeis, *Analyst*, 2007, **132**, 507–511.
8 R. Narayanaswamy and O. S. Wolfbeis, *Optical sensors: industrial environmental and diagnostic applications*, Springer Science & Business Media, 2013, vol. 1.
9 J. H. Lee, Z. Wang, J. Liu and Y. Lu, *J. Am. Chem. Soc.*, 2008, **130**, 14217–14226.
10 G. I. Vargas-Zúñiga and J. L. Sessler, Sensors for Lanthanides and Actinides- *The Rare Earth Elements*, Wiley & Sons, 2012.
11 J. L. Sessler, P. J. Melfi, D. Seidel, A. E. V Gorden, D. K. Ford, P. D. Palmer and C. D. Tait, *Tetrahedron*, 2004, **60**, 11089–11097.
12 E. Rabinovich, S. Aharonovich, M. Botoshansky and M. S. Eisen, *Dalt. Trans.*, 2010, **39**, 6667–6676.
13 J. P. Frick, *Woldman's engineering alloys*, ASM international Materials Park, OH, 1994.
14 R. Martin, *Super Fuel (Thorium, the Green Energy Source for the Future)*, 2013.
15 C. M. West, *Health Phys.*, 1962, **8**, 279–297.
16 World Health Organization. *Guidelines for drinking water quality: radiological aspects*, 2004.
17 P. Shrivastav, S. K. Menon and Y. K. Agrawal, *J. Radioanal. Nucl. Chem.*, 2001, **250**, 459–464.
18 A. W. Al-Shawi and R. Dahl, *J. Chromatogr. A*, 1995, **706**, 175–181.
19 K. H. Theimer and V. Krivan, *Anal. Chem.*, 1990, **62**, 2722–2727.
20 N. Soltani, H. Haddadi, M. Asgari and A. Semnani, *J. Radioanal. Nucl. Chem.*, 2015, **304**, 603–607.
21 M. R. Ganjali, P. Norouzi, F. Faridbod, S. Riahi, M. R. Yaftian, A. Zamani and D. Matt, *J. Appl. Electrochem.*, 2007, **37**, 827–

833.
22 W. J. Campbell and H. F. Carl, *Anal. Chem.*, 1955, **27**, 1884–1886.
23 M. S. De Carvalho, M. De LF Domingues, J. L. Mantovano and J. Da Cunha, *J. Radioanal. Nucl. Chem.*, 2002, **253**, 253–256.
24 J. C. Veselsky, B. Kwiecinska, E. Wehrstein and O. Suschny, *Analyst*, 1988, **113**, 451–455.
25 C. W. Sill, *Anal. Chem.*, 1977, **49**, 618–621.
26 A. Murray, R. Marten, A. Johnston and P. Martin, *J. Radioanal. Nucl. Chem.*, 1987, **115**, 263–288.
27 L. Ye and C. A Lucy, *Talanta*, 1996, **43**, 811–817.
28 D. Wu, A.C. Sedgwick, T. Gunnalaugsson, E.U. Akkaya, J. Yoon and T.D. James, *Chem. Soc. Rev.,* 2017, **46**, 7105-7123.
29 O. S. Wolfbeis, *Angew. Chemie Int. Ed.*, 2013, **52**, 9864–9865.
30 R. Gao, J. Hu, K. Zhang, Y. He, P. Liu, S. Luo, Y. Yang, L. Yang, W. Feng and L. Yuan, *Chinese J. Chem.*, 2013, **31**, 689–694.
31 J. Wen, L. Dong, J. Tian, T. Jiang, Y.Q. Yang, Z. Huang, X.Q. Yu, C.W. Hu, S. Hu and T.Z. Yang, *J. Hazard. Mater.*, 2013, **263**, 638–642.
32 B. K. Rani and S. A. John, *New J. Chem.*, 2017, **41**, 12131–12138.
33 C. G. Frankær and T. J. Sorensen, *Analyst*, 2019, **144**, 2208-2225.
34 P. Bühlmann, E. Pretsch and E. Bakker, *Chem. Rev.*, 1998, **98**, 1593–1688.
35 R. Selva Kumar, S. K. Ashok Kumar, K. Vijayakrishna, A. Sivaramakrishna, C. V. S. R. Brahmmananda, N. Sivaraman and S. K. Sahoo, *Inorg. Chem.*, 2018, **57**, 15270–15279.
36 I. Murkovic and O. S. Wolfbeis, *Sensors Actuators B Chem.*, 1997, **39**, 246–251.
37 A. Safavi and M. Sadeghi, *Anal. Chim. Acta*, 2006, **567**, 184–188.
38 O. Gumrah, N. Malcik and P. Caglar, *Sensors Actuators B Chem.*, 2009, **139**, 125–131.
39 S. Rastegarzadeh, N. Pourreza and I. Saeedi, *J. Hazard. Mater.*, 2010, **173**, 110–114.
40 L. M. Trutneva, O. P. Shvoeva and S. B. Savvin, *Zhurnal Anal. Khimii*, 1989, **44**, 1804–1808.
41 M. K. Mahani, F. Divsar, M. Chaloosi, M. G. Maragheh, A. R. Khanchi and M. K. Rofouei, *Sensors Actuators B Chem.*, 2008, **133**, 632–637.
42 A. Safavi and M. Sadeghi, *Anal. Chim. Acta*, 2006, **567**, 184–188.
43 A. A. Elabd, *RSC Adv.*, 2016, **6**, 45525–45532.
44 O. S. Wolfbeis, *Fiber optic chemical sensors and biosensors*, CRC, 1991, vol. 1.
45 T. J. Sørensen, M. Rosenberg, C. G. Frankær and B. W. Laursen, *Adv. Mater. Technol.*, 2019, **4**, 1800561-7.
46 R. Selvakumar, S. K. Ashok Kumar, K. Vijayakrishna, A. Sivaramakrishna, C. V. S. Brahmmananda Rao, N. Sivaraman and S. K. Sahoo, *Sensors Actuators B Chem.*, 2017, **255**, 1391–1400.
47 R. Selva Kumar, S. K. Ashok Kumar, K. Vijayakrishna, A. Sivaramakrishna, C. V. S. B. Rao, N. Sivaraman and S. K. Sahoo, *Spectrochim. Acta Part A Mol. Biomol. Spectrosc.*, 2019, **214**, 32–39.
48 R. Selva Kumar, S. K. Ashok Kumar, K. Vijayakrishna, A. Sivaramakrishna, C. V. S. B. Rao and N. Sivaraman, *Anal. Methods*, 2019, **11**, 1338-1345.
49 G. T. Alok K. Bhattacharya, *Chem. Rev.*, 1981, **81**, 415–430.
50 C. Würth, M. Grabolle, J. Pauli, M. Spieles and U. Resch-Genger, *Nat. Protoc.*, 2013, **8**, 1535.
51 A. M. Brouwer, *Pure Appl. Chem.*, 2011, **83**, 2213–2228.
52 R. Selva Kumar, S. K. Ashok Kumar, K. Vijayakrishna, A. Sivaramakrishna, P. Paira, C. V. S. B. Rao, N. Sivaraman and S. K. Sahoo, *New J. Chem.*, 2018, **42**, 8494–8502.
53 U. Fegade, S. Attarde and A. Kuwar, *Chem. Phys. Lett.*, 2013, **584**, 165–171.
54 W.H. Ding, D. Wang, X.J. Zheng, W.J. Ding, J.Q. Zheng, W.H. Mu, W. Cao and L.P. Jin, *Sensors Actuators B Chem.*, 2015, **209**, 359–367.
55 A. P. De Silva, H. Q. N. Gunaratne, T. Gunnlaugsson, A. J. M. Huxley, C. P. McCoy, J. T. Rademacher and T. E. Rice, *Chem. Rev.*, 1997, **97**, 1515–1566.
56 P. Job, *Ann. di Chim. Appl.*, 1928, **9**, 113–203.
57 B. Valeur and M. N. Berberan-Santos, *Molecular fluorescence: principles and applications*, John Wiley & Sons, 2012.
58 A. V. Hill, *J. Physiol.*, 1910, **40**, 4–7.
59 M. Shamsipur, T. Poursaberi, M. Hassanisadi, M. Rezapour, F. Nourmohammadian and K. Alizadeh, *Sensors Actuators, B Chem.*, 2012, **161**, 1080–1087.
60 M. Shamsipur, M. Hosseini, K. Alizadeh, N. Alizadeh, A. Yari, C. Caltagirone and V. Lippolis, *Anal. Chim. Acta*, 2005, **533**, 17–24.
61 G. L. Long and J. D. Winefordner, *Anal. Chem.*, 1983, **55**, 712A-724A.
62 C. Moulin, B. Amekraz, S. Hubert and V. Moulin, *Anal. Chim. Acta*, 2001, **441**, 269–279.